

7-2-1987

## Secondary Electron Emission Induced by Electron Bombardment of Polycrystalline Metallic Targets

R. Bindi  
*Université de Nice*

H. Lanteri  
*Université de Nice*

P. Rostaing  
*Université de Nice*

Follow this and additional works at: <https://digitalcommons.usu.edu/microscopy>



Part of the [Biology Commons](#)

---

### Recommended Citation

Bindi, R.; Lanteri, H.; and Rostaing, P. (1987) "Secondary Electron Emission Induced by Electron Bombardment of Polycrystalline Metallic Targets," *Scanning Microscopy*. Vol. 1 : No. 4 , Article 1. Available at: <https://digitalcommons.usu.edu/microscopy/vol1/iss4/1>

This Article is brought to you for free and open access by the Western Dairy Center at DigitalCommons@USU. It has been accepted for inclusion in Scanning Microscopy by an authorized administrator of DigitalCommons@USU. For more information, please contact [digitalcommons@usu.edu](mailto:digitalcommons@usu.edu).



SECONDARY ELECTRON EMISSION INDUCED BY ELECTRON BOMBARDMENT  
OF POLYCRYSTALLINE METALLIC TARGETS

R. Bindi\*, H. Lanteri and P. Rostaing

Laboratoire d'Emission Electronique  
et de Luminescence  
Université de Nice - Parc Valrose  
06034 - Nice - Cedex - France

(Received for publication January 31, 1987, and in revised form July 02, 1987)

Abstract

The aim of the present paper is the analysis of the backward secondary electron emission phenomenon, under electron bombardment, on the basis of experimental and theoretical results. Among the theoretical models, we will mention the phenomenological models, those which use a Monte-Carlo type simulation method, and those based on the numerically solved Boltzmann transport equation.

To correlate experimental and theoretical results on all the data characterizing this phenomenon, it is necessary to use an appropriate description for the excitation process of the internal secondary electrons; it also needs a complete description of the transport process for the excited electrons, which incorporates the elastic and inelastic interactions, as well as the energy and angular distribution of the incident primary beam.

From this, it follows that it will be necessary, either to use a "direct" Monte-Carlo simulation method, or, in the case of the transport model, to carry out a preliminary treatment of the primary electron dispersion; this treatment is also based upon a Boltzmann equation resolution.

The results of such an analysis will be useful in electron microscopy and in quantitative Auger spectroscopy.

Key Words: Secondary electron emission, secondary yield, secondary electron distribution, back-scattered electrons, elastic scattering, inelastic scattering, transport equation, Monte-Carlo simulation.

\*Address for correspondence:

R. Bindi, Laboratoire d'Emission Electronique et de Luminescence - Université de Nice, Parc Valrose - 06034 Nice Cedex - France  
Phone No. (33) 93-52 98 98 x 9658

Introduction

When a solid is bombarded by an electron beam, the incident electrons diffuse in the solid as a result of elastic and inelastic collisions. In this process, energy losses occur which give rise to X rays and secondary electrons, as well as heat dissipation. For values of the primary energy lower than a few keV, the secondary electron emission (SEE) is the dominant phenomenon.

The excited electrons in the bulk of the material, produced by the incident primary electrons, are the internal secondary electrons which themselves produce on their path, other secondary electrons. A cascade process is the net result of these successive collisions.

Then, the number, the energy and angular distributions of the secondary electrons reaching the surface with sufficient energy to overcome the potential barrier, are determined by the excitation process and by the diffusion mechanisms.

We will devote our present paper to the backward SEE of polycrystalline metals bombarded by a monoenergetic electron beam with an energy less than 3 keV and under normal incidence.

First, we will recall, the main data of this phenomenon, then we will describe, the most important physical processes occurring in SEE. We will review the main theoretical models used in this field of research, indicating in particular the way the above mentioned processes are treated by each of these models.

Characteristic data of the SEE

Given the large number of review papers (24, 32,49,57,58) on this subject, we will dwell only on the principal data of the phenomenon, under the previously mentioned conditions.

Energy distributions of the secondary electrons

A typical curve of the energy distribution of the emitted electrons is shown in fig. 1.

Although it is common to call "secondary electrons" all the emitted electrons, one may distinguish between three categories of electrons leaving the surface:

- Elastically reflected primaries, characterized by a sharp peak at the primary energy (Region 3). The number of such electrons is very low.
- Inelastically reflected primaries or backscat-

tered electrons (Region 2). These electrons which lose a part of their energy by exciting lattice electrons, go back and escape from the surface as a result of scattering.

- "True" secondaries. The majority of the emitted electrons have low energies, corresponding to the broad peak (Region 1). The maximum of this peak lies for most solids in the vicinity of a few eV. The electrons whose energy is lower than 50 eV are called "True secondary electrons". They are mainly electrons which originally occupied bounded states within the metal. The shape of the peak varies with the target material and, in many cases, presents fine structures (56,95,112). Increasing the incident electron energy, the full width at half maximum decreases and, the peak position shifts towards lower energies, until a steady state is reached (11,38,105).

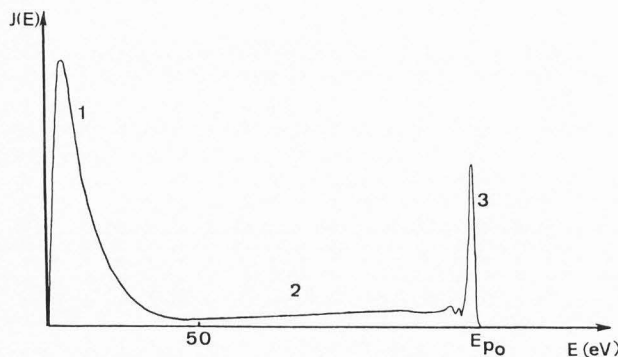


Figure 1. Energy spectra of secondary electrons  
 1 - True secondary electrons  
 2 - Backscattered electrons  
 3 - Elastically reflected electrons.

Secondary emission yield

The total yield  $\delta_{tot}$ , may be defined as the ratio of the total number of emitted electrons to the number of primary electrons impinging on the solid. In this way, the total yield includes the three categories of emitted electrons previously mentioned. Neglecting the elastically reflected primary electrons, we can write :

$$\delta_{tot} = \delta_{true} + \eta \quad (1)$$

where  $\delta_{true}$  is the ratio of the number of the true secondary electrons to the number of incident electrons and  $\eta$  is the ratio of the number of backscattered electrons, with energies higher than 50 eV, to the number of incident electrons.

One of the most important relationships in SEE is that which exists between the secondary yield  $\delta_{true}$  and the energy  $E_{p0}$  of the incident primaries. For all materials,  $\delta_{true}$  increases with  $E_{p0}$  then goes through a maximal value and finally decreases for high primary energies (11,16,18,19, 20,105,123).

Maximal true secondary electron escape depth

This parameter is experimentally obtained by measuring the yield variations or energy distribution shifts as a function of thin film thicknesses for a metal deposited on a substrate of another metal. During these experiments the energy of the primary beam is fixed. The values thus obtained

are about 20 monolayers, viz, 5 nm (18,22,87,91).  
Effect of backscattered electrons on SEE

For high enough primary energies one can consider that the 5 nm surface layer previously mentioned is crossed by two flows of electrons : the forward primary beam and the backward inelastically reflected electrons (backscattered electrons). If we denote by  $\delta_0$  the yield of secondary electrons produced directly by the primary beam, and by  $\delta_1$  the yield of these produced by backscattered electrons, we can write :

$$\delta_{true} = \delta_0 + \delta_1 \quad (2)$$

The measurements of these two contributions  $\delta_0$  and  $\delta_1$  are important, for example, in electron microscopy for the image quality determination. Experimentally  $\delta_0$  and  $\delta_1$  can be determined with the help of the method describe in (21,22) based on the use of the  $\delta_{true}(\eta)$  diagrams. These diagrams are derived from  $\delta_{true}$  and  $\eta$  measurements on targets prepared as described in the previous section. For thicker targets, the yield  $\delta_{true}$  can be written in the form :

$$\delta_{true} = \delta_0 + C \eta \quad (3)$$

where "C" is the mean backscattered electron effectiveness for secondary electron production ; it is then given by the value of the slope of the  $\delta_{true}(\eta)$  curve.

In Table 1 all the values of C and  $\frac{C}{\delta_0}$  (comparative yield for the production of a true SE between backscattered and primary electrons) are grouped as a function of the energy of the primary beam for Al and Au (17,18,79,116,123).

Among the most important causes of eventual discrepancy between experimental values, one can mention : target pollution, conditions for the utilization of the analysis systems (70,76,93) and target nature (bulk or evaporated thick films).

Table 1. Experimental values of the effectiveness C of backscattered electrons. a) Aluminium ; b) gold.

(a)

$E_{p0}$ (keV)	0.6	0.8	1	1.5	2	Ref
C	1.8	1.6	1.45	1.15	1	(79)
$C/\delta_0$	7	6.3	5.9	5.5	0.76	(18)(17)
		6.8	6.3	4.8	5.85	(79)
					3.8	(18)
						(123)

(b)

$E_{p0}$ (keV)	1.85	2	2.2	2.4	2.6	Ref
C	1.62	1.63	1.36	1.27	1.16	(79)
$C/\delta_0$	3.9	4.2	2.9	2.8	2.5	(17)

See page 1485 for symbol table.

Angular distribution

In polycrystalline targets, the external angular distribution of the true secondary electrons is very close to a cosine law (63,66) which is nothing else but a result of the complete diffusion state of internal electrons or, in other words, of an isotropic angular distribution of these electrons.

The previously mentioned data are generally obtained directly from experiment. However, even more information concerning SEE, to the understanding and to the analysis of the processes occurring in this phenomenon, can be provided by SEE measurements on thin films evaporated on bulk metal or self supporting. In his paper, Jahrreiss (62) collected all the data accessible by these methods such as, for example, the true secondary electron escape depth, and the effectiveness of backscattered electrons on true secondary electrons yield, the role of which has been emphasized by Kanter (68) and Palmberg (92).

Elementary processes in SEE

Most important among the processes acting during SEE, are the individual and collective inelastic interactions of an electron with the electron gas in the solid (the jellium), the inelastic interactions with the inner shell electrons and the elastic interactions with the core ions (Radium). Touzillier (126) showed that the role of phonons in metals is negligible in SEE.

Inelastic interactions lead to the creation of so called internal secondary electrons either directly, or as a consequence of the decay of plasmons generated by high-energy incident electrons. Interactions with inner shell electrons play an important role in the slowing down of primary electrons. Elastic interaction is prominent in the angular dispersion.

Interaction with jellium

In normal metals. They are those such as Al, to which the quasi-free electron approximation applies,

a) Lindhard's dielectric function. The study of the interaction of an incident electron with the free electrons of a solid, leading to a transfer of energy  $\hbar\omega$  and momentum  $\hbar\mathbf{q}$ , is carried out by the use of the non-interacting infinite electron gas model. The assumed linear interaction of such a medium to an external perturbation due to an electron having an energy above a certain level, leads in the random phase approximation (R.P.A.) to the longitudinal dielectric function  $\epsilon(\mathbf{q},\omega)$  of the solid. The expression most currently used is the Lindhard's dielectric function (81). The latter is a complex function which, in fact, depends only on  $\mathbf{q}$ 's modulus and which can be separated into real and imaginary parts :

$$\epsilon(\mathbf{q},\omega) = \epsilon_1(\mathbf{q},\omega) + i\epsilon_2(\mathbf{q},\omega) \quad (4)$$

We recall (fig. 2) the properties of this function. The individual excitations lie in the interval where  $\epsilon_2$  is non zero. The limits of this interval are two parabola whose equations are derived from the law of energy and momentum conservation.

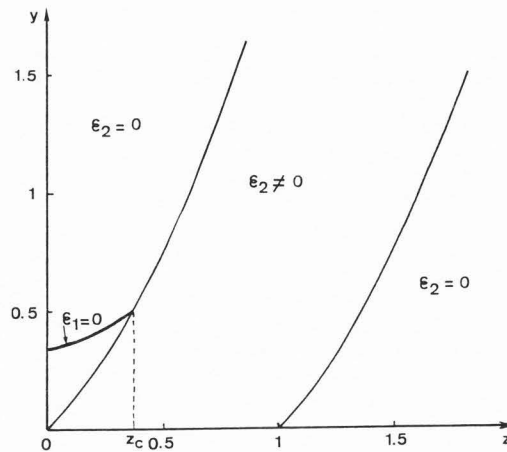


Figure 2. Energy of excitations shown as function of momentum from Lindhard's dielectric function  $y = \frac{\hbar\omega}{4E_F}$ ,  $z = \frac{q}{2k_F}$ ,  $z_c$  cutoff value for plasmon excitation,  $\hbar q$  is the momentum transfer,  $\hbar\omega$  is the energy transfer,  $\hbar k_F$  and  $E_F$  are the Fermi momentum and energy, respectively.

For low values of  $z$ , and therefore of  $q$ , where  $\epsilon_2$  is zero, the  $\epsilon_1$  function becomes equal to zero for discrete values of the energy  $y$ . Then the loss function  $\text{Im}(-\frac{1}{\epsilon}) = \frac{\epsilon_2}{\epsilon_1^2 + \epsilon_2^2}$  has a pole. This indicates the existence of collective excitation. The  $z$  dependent  $y$  values, for which  $\epsilon_1$  is zero give the typical dispersion characteristic of the bulk plasmon.

The general aspect of the loss function, for different values of  $z$ , is represented in fig. 3. In all cases, the arrow indicating the position of the bulk plasmon is seen to be well outside the range of the individual interactions.

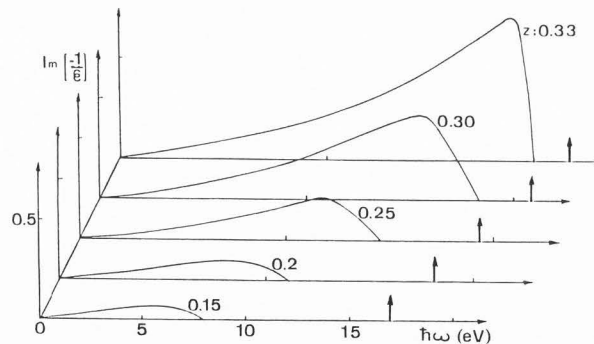


Figure 3. Lindhard loss function  $\text{Im}(-\frac{1}{\epsilon(\omega,\mathbf{q})})$  versus energy transfer. The arrows  $\uparrow$  are Dirac's functions and indicate the positions of the volume plasmons.

b) Mermin's dielectric function. A number of corrections can be introduced in order to take into account, in an approximate way, correlation and exchange effects like (5,23,34,50,119,120) and particularly the finite life time of the elementary excitations (69). This leads to Mermin's

dielectric function (88). Thus, dissipative processes such as energy losses due to phonon scattering or diffusion by all kinds of defects found in real metals, may be taken into account, by means of a damping factor.

This leads, in the case of collective interactions, to a broadening of the plasmon resonance line as well as a modification of the dispersion relation and of the m.f.p. (mean free path). Zacharias (134,135) and Ashley and Ritchie (3), among others, analysed these phenomena.

In Mermin's dielectric function (fig. 4), there is no explicit separation between individual and collective processes. For low "z" values (low q values), the pronounced sharpness of the loss function is assigned essentially to collective excitations, according to the experimental values of the characteristic energy losses. For higher "z" values, the plasmon peak is increasingly masked by individual contributions.

The infinite electron gas model is convenient in describing bulk processes which are dominant in SEE while a semi-infinite electron gas model also takes into account surface excitations (44).

Noble metals (Ag, Au, Cu). For these metals, the "d" electrons can participate in conduction phenomena. The "jellium" must be redefined (27). The dielectric theory of electron gas cannot be

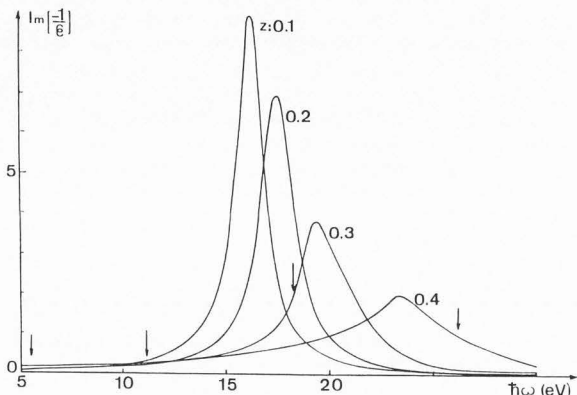


Figure 4. Mermin loss function. The arrows indicate the separation between individual and collective excitations according to Lindhard's dielectric function.

applied here. A complete theoretical calculation of the dielectric function does not exist. Hence, we used an experimental function deduced from transmission energy loss measurements. These measurements are carried out along the axis normal to the surface. Due corrections are made to eliminate the effects of multiple losses and of surface interactions (40,101,131) and  $\epsilon(0,\omega)$  is thus obtained. Following the conclusions of Nagel and Witten (90), bearing on the weak q dependence of the loss function, Ganachaud (44) proposed a separable form for  $\epsilon(q,\omega)$

$$\epsilon(q,\omega) = (1 + aq) \cdot \epsilon(0,\omega) \quad (5)$$

where a is a constant.

In the limiting case, when  $q \sim 0$ , both longitudinal and transverse dielectric constants can be considered to have the same value, thus justifying the use of the experimentally obtained optical constant for the dielectric constant (7,94).

We can see on figure 5, in the case of Cu, that the Wehenkel's loss function (131) is very close to that of Feldkamp et al. (40). The most pronounced peak, corresponding to a 20 eV energy loss, can be assigned to collective excitations.

However, collective excitation does not appear clearly in the  $\epsilon_1$  and  $\epsilon_2$  curves calculated from the loss functions.

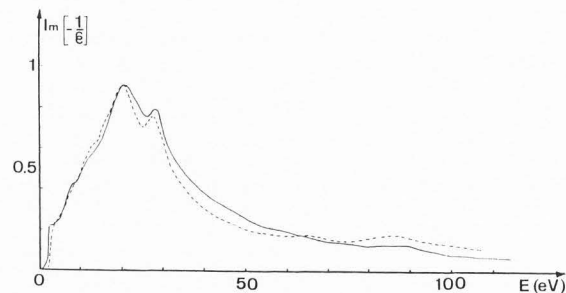


Figure 5. Energy loss function of copper. Full line (131), dashed line (40).

Physical data obtained from dielectric theory

The knowledge of dielectric loss function permits one to obtain: a) the creation rate of internal secondary electrons due to individual interactions or the plasmon decay by electron-hole pair creation, b) the differential cross section and the m.f.p. for interactions of an electron (energy E) yielding an amount of energy  $\hbar\omega$  and momentum  $\hbar q$  to the electron gas.

Under the restriction of energy and momentum conservation rules, these data are obtained from the expression

$$W(\vec{q},\omega) = \frac{8 e^2}{\hbar q^2} \text{Im} \left[ - \frac{1}{\epsilon(\vec{q},\omega)} \right] \quad (6)$$

Here  $W(\vec{q},\omega)$  is the probability per unit time for an electron to yield an amount of energy  $\hbar\omega$  and momentum  $\hbar q$  to the solid.

Interaction with inner shell electrons

The excitation of the inner electronic levels of atoms is one of the main mechanisms responsible for the energy losses of charged particles. In spite of their low occurrence probability, these interactions are the most important in the slowing down of the primary beam.

The theoretical and experimental data most frequently found in literature are related to the creation by electron bombardment of a vacancy, especially in the K and L shells. An analysis of these data has been carried out by many authors such as Powell (96), Estrade (37) and Ganachaud (44).

In the various treatments of the inner shell electron excitation only the direct transitions between a bound state and a state in the continuum are considered. Tung and Ritchie (127) showed that transitions towards discrete energy states may be neglected. Furthermore the inner shell binding energies are assumed to be practically the same as those of the isolated atom. Finally,

the creation of multiple vacancies during a single collision is not considered. In the SEE investigations energy range, the role of the K shell can be neglected and no relativistic corrections are needed. Among the numerous descriptions of the ionization of an atom, one can mention: Bethe's expression, classical and quantum theories, empirical formulas, and experimental values. Using the Born approximation, Bethe (9) obtained for the atomic ionization cross section, an expression which contains several parameters the values of which are obtained by a comparison either with other calculations, or with experimental data. This expression is suitable for high energy incident electrons. The cross section  $\sigma_{nl}$  is written:

$$\sigma_{nl} E_{nl}^2 = \frac{2\pi e^4}{U_{nl}} Z_{nl} b_{nl} \ln \left( c_{nl} U_{nl} \right) \quad (7)$$

with  $U_{nl} = \frac{E_0}{E_{nl}}$ , and where  $E_0$  is the incident electron energy;  $E_{nl}$  the binding energy for the  $nl$  shell;  $Z_{nl}$  the number of electrons of the  $nl$  shell;  $b_{nl}$  and  $c_{nl}$  the unknown parameters previously mentioned.

In the quantum mechanical models (4,60) the cross sections are deduced from generalized oscillator strengths. Thus, Mac Guire (84) has calculated  $L_1$ ,  $L_{23}$  and  $M$  ionization cross sections for low atomic number  $Z$  ( $< 18$ ) materials. Manson (85) has calculated the  $L$  shell ionization cross section for Al, using the Hartree-Slater central field model. The better results are obtained for the higher values of the impinging particles energy. The accuracy is limited by the choice of the wave functions used for the initial and final states of the target-atom. Many computations are carried out using simple hydrogenic initial states. This approach is probably justified for the K shell, but it is not realistic for the L shell and definitely wrong for the higher shells.

Among the classical formulations we can mention those of Burgess and Percival (25), Vriens (130) and especially those of Gryzinski (52,53, 54) who uses the Coulomb collision model for two moving particles. The latter theory seems the most frequently used. In such a formulation, the differential cross section for an electron of energy  $E$ , yielding an energy  $\Delta E$  to an inner shell electron, is given by:

$$\sigma(\Delta E, E, U_i) = \frac{\sigma_0}{(\Delta E)^3} g_\sigma \left( \frac{U_i}{E}, \frac{E}{\Delta E} \right) \quad (8)$$

with  $\sigma_0 = 6.56 \text{ (eV)}^2 \text{ (nm)}^2$ , energies expressed in eV,  $U_i$  identified with the binding energy of an  $i$  shell electron.

Setting  $X = \frac{E}{U_i}$  and  $Y = \frac{\Delta E}{U_i}$ ,  $g_\sigma$  can be written:

$$g_\sigma(X, Y) = \frac{1}{X(1+X)}^{3/2} \left[ Y \left( 1 - \frac{1}{X} \right) + \frac{4}{3} \ln \left[ 2.718 + (X-Y)^{1/2} \right] \right] \cdot \left( 1 - \frac{Y}{X} \right)^{1/1+Y} \quad (9)$$

Several semi-empirical formulae were also given by Drawin (36) and Lotz (82).

Three experimental methods are used for the ionization cross section measurements. One is based on the absolute yield measurement of characteristic X-ray lines for a target bombarded by electrons. Another starts from the characteristic Auger electron yield. The third one is based on the characteristic energy losses. There are plenty of results for the K shell (31,114). They are rather rare for the L shell (114) and quite lacking for the M shell.

Comparison between the various theoretical approaches and experiment led Powell (96), Estrade (37) and Ganachaud (44) to the conclusion that a good agreement is obtained for the K shell ionization cross sections, while a greater discrepancy characterizes the L shell. Thus, as pointed out by Ganachaud (44) the values of the total cross section given by Gryzinski's approximation are about 25 % lower than the experimental results. Furthermore, the theoretical spectrum of the energy losses, due to ionization of L or higher inner shells, given by Gryzinski decreases monotonously from the threshold value to the maximum loss value. In contrast, in the case of experimental results, the most probable energy loss is situated above the threshold value. Manson's calculations give a better agreement for the energy loss spectra.

#### Elastic collisions

The elastic scattering process of incident electrons with the core-ion randomly distributed in the solid is the dominant process in the angular deviation of the electrons. One can show theoretically that, during the inelastic process, the probability of a large angle scattering is very low. On the other side, the backscattered electron energy spectra show energy lines corresponding to characteristic energy losses due to plasmon creation. If such electrons suffering a single inelastic collision are, after a reversal of direction, reemitted outside the solid, one is compelled to accept that they also suffer one or more large angle elastic collisions. This points out the leading role of the elastic scattering on the angular deviation. Thus, it is necessary to define carefully the differential cross section related to this scattering process.

Rutherford cross section. For metals with low  $Z$  atomic number, and for energies above 1 keV, Rutherford's screened cross section is widely used to describe the elastic process; we can write:

$$\sigma_{e1}(E, \alpha) = \frac{Z^2 e^4}{4E^2} \frac{1}{(1 - \cos \alpha + 2\xi)^2} \quad (10)$$

where  $E$  is the electron energy,  $Z$  the atomic number,  $\alpha$  the scattering angle,  $e$  the electron charge and  $\xi$  a screening parameter. However, as pointed out by Krefting and Reimer (73), this cross section is only a very rough approximation, and therefore, not suitable in the case of heavy metals (61).

Cross sections given by the partial wave method. More realistic cross sections may be calculated by the partial wave method (74,128).

An elastic collision can be described as a scattering of a reduced mass particle in the field  $U(r)$  of a fixed central force. The partial wave method is based on the comparison between the steady states, whose angular momentum is defined in the potential  $U(r)$  (partial waves), and the analogous steady states in the absence of potential (free spherical waves).

The difference between a "partial wave" and the "free spherical wave" with an angular momentum "l" is characterized by a phase shift " $\delta_l$ ". In order to calculate the cross sections by means of the phase shifts, it is sufficient to know, how the "scattering steady states" can be built up with the aid of the partial waves. A comparison between these two types of differential cross sections, for several metals, was carried out by Ichimura et al (61) and Valkealahti and Nieminen (128).

#### Theoretical models for SEE

The greatest obstacle in a satisfactory description by the theoretical models lies in the fact that they do not embrace simultaneously all the different elementary processes. Thus, most of the models treat only one special aspect of the phenomenon ; the proposed models could be classified as follows :

- phenomenological theories
- quantum mechanical models for SE production
- transport models
- simulation models.

#### Phenomenological theories

These models initially developed by Baroody (6) and Jonker (67), were able to explain the general behaviour of the secondary emission yield curve as a function of the primary beam energy. In these theories, one makes the assumption that the number of created internal electrons is proportional to the energy loss per unit path length of the incident electron. The stopping power laws, used in this case, which takes into account all the inelastic processes experienced by the primary electrons, are experimental laws deduced from range measurements (115,42).

These laws are generally written in the form:

$$\frac{dE_p}{dx} = - A E_p^{n-1}(x) \quad (11)$$

where  $E_p(x)$  is the primary electron energy at depth  $x$ ,  $A$ , a constant, depending on the material, and  $1.3 < n < 1.6$ .

The diffusion and the escape into the vacuum of the secondary electrons generated at depth  $x$  is described by means of an exponential absorption law. The best results are obtained if a constant "energy loss" law of the primary electrons (83), and an isotropic angular distribution of the internal secondary electrons is assumed (27,35). The assumption of a constant "energy loss" law is a way to taking into account the primary electrons dispersion (133), while the choice of an isotropic angular distribution is being accounted for by the influence of backscattered electrons. These simple theories give a universal yield curve. This theoretical curve shows considerable deviation from the experimental one's at large values of primary

energies. Furthermore the distinction between total yield  $\delta_{tot}$  and true secondary yield  $\delta_{true}$  is not well established and no information is given on energy and angular distribution of secondary electrons.

#### Quantum mechanical theories of secondary electron creation

In these models, an analysis is made of primary electron (assumed to be free) individual interactions with lattice electrons. From relation (6), one can calculate the transition probability of an inner lattice electron to an excited state (33,41,129). Thus, in the free electron approximation, Streitwolf (122) calculated the energy and angular distributions of internal secondary electrons ; the latter shows a strong anisotropy. Thus, the isotropic behaviour, experimentally observed for the internal angular distribution cannot be explained by this model. Furthermore, as shown by Cailler (27), the free electrons approximation fails when "d" electrons participate in the secondary emission process ; this is the case in the noble metals. The results given by these models are frequently used as a source term for the description of internal secondary electrons diffusion.

By the use of an exponential function, as in the phenomenological theories, and their assumptions therein, for the description of the internal secondary electron scattering, Chung and Everhart (29,30) using free electron gas model, developed a theoretical calculation of the energy distribution taking or not taking into account the quantum reflection effect at the solid-vacuum interface (28). In this model :

- the primary electron is assumed to travel along a straight line defined by its initial direction; this approximation is valid for high values of the primary beam energies ;
- the excitation process is assumed to be isotropic ; this is justified by taking into account of the primary beam dispersion.

In their treatment of the SE transport and escape problem, they only consider those SE's that do not suffer any scattering on their way to the surface, and those that scatter only once. The shape of the energy distribution thus obtained does not depend on the energy of the primary beam. One of the important features of this model is the introduction in the absorption process of an energy dependent m.f.p. as brought out by the works of Quinn (100), and Ritchie and Ashley (104).

#### Transport theories

In these models, the SEE phenomenon can be separated into the following processes :

- penetration and diffusion of the incident electrons within the material
- excitation of the target electrons by the primary beam electrons
- transport towards the surface of the internal secondary electrons
- crossing of the potential barrier.

Boltzmann's transport equation is applied to the scattering of the internal secondary electrons towards the surface. Wolff (132) was the first one to propose a model based on the equation used by Marshak (86) in neutron scattering.

In the steady state and in the absence of external forces, the equation can be written :

$$\vec{v} \cdot \vec{\nabla}_{\vec{r}} N(\vec{r}, \vec{p}) = \sum_i Q_i(\vec{r}, \vec{p}) \quad (12)$$

where  $N(\vec{r}, \vec{p})$  is the electron density at the point  $\vec{r}$  in the solid,  $\vec{p}$  the momentum,  $\vec{v}$  the electron velocity and  $Q_i(\vec{r}, \vec{p})$  the rate of variation of the density for a given process.

For a target bombarded at normal incidence and under the assumption that the density of the internal secondary electrons depends only on the depth, each term of the equation is expressed as a function of the depth, of the angle  $\theta$  defining the propagation direction relative to the inward normal and of the electron energy  $E$ . The crossing of the potential barrier is generally treated by considering the exit cone and a specular reflection outside the cone.

The various models based on the use of the Boltzmann equation differ one from the other by the choice of :

- the excitation function by primary electrons with or without the contribution of backscattered electrons
- the inelastic collisions terms
- the simplifying assumptions made according to the solving method, analytic or numerical.

Attempts to find analytic solutions of the integro-differential equation initially failed to encompass and to correctly describe all the elementary processes. Puff (97,98,99) developed a method of analytic solution for the case of isotropic excitation and dispersion, assuming the excitation to occur either at the end of or along the path of the primary electrons.

Streitwolf (122) treated the transport process by the partial wave method under both assumptions : i) an anisotropic excitation, which is characteristic of the individual interactions in the free electrons approximation and ii) an initial direction maintained for the primary beam. Moreover, if the depth dependence is neglected, the splitting of the partial waves is obtained, thus making easier the mathematical solution.

Amelio (1,2), extending Stolz's (121), Guba's (55) and Grinchak's (51) works, applied this method by adding to the electron-electron scattering, a contribution due to electron-plasmon interaction. Amelio used Streitwolf's source function and a variation by steps of the ratio between the electron-plasmon and electron-electron m.f.p., as a function of energy. A certain number of corrections to Amelio's theoretical work have been introduced by Moulin et al. (89).

An analysis of the results deduced from the above models, suggests the following remarks :

a) concerning the yield :

The slowing down of the primary electron was neglected. The effect of their angular dispersion on the source function was only taken into account in a very approximate way, by the isotropy assumption of the excitation process. So, only the primary electron action during the penetration was described. As a consequence,  $\delta_0$  is the only theoretical parameter comparable to experiment. In the case of an individual excitation, obtained values of  $\delta_0$  are one order of magnitude too low for Al,

and two orders for Au (102,103). Therefore, in the excitation process of SEE, one has to consider the bulk plasmon damping in metals such as Al, and the "d" electrons contribution of the noble metals (26,27).

b) concerning energy distributions :

- To obtain values of f.w.h.m., comparable to experimental ones, one has to take into account the variation of the m.f.p. with energy.

- The partial wave splitting does not describe perfectly the energy distribution variations with primary energy ; Puff's theory gives a better agreement.

c) concerning angular distribution :

The strong anisotropic character of the individual excitation process is not sufficiently reduced by the transport process.

In conclusion, these models offer no satisfactory description of SEE. The poor results obtained are due to the numerous simplifying assumptions made necessary by the mathematical complexity of the equation used.

The improvement of numerical treatment of integro-differential equations, following the quick growth of power in computers, made it possible to reformulate and to solve, in a more satisfactory way, Boltzmann's equation applied to SEE. Bennett and Roth (8) have thus been able to introduce the influence of the primary beam dispersion into the source function. These authors adopted Wolff's (132) analysis for the SE transport process.

Later, more complete theoretical models were developed by Bindi et al. (13,14), Schou (113) and Rösler et al. (106,107). The models of Bindi et al. and Rösler et al. take into account all possible creation processes of SE resulting from the interaction of primary electrons with free as well as bound electrons (106,107) and from the bulk plasmon decay. In the description of the inner SE transport, elastic scattering is now introduced in addition to the inelastic one. The justification of the elastic process importance results from the comparison of the respective values of the elastic and inelastic m.f.p. However, Rösler et al. neglect the depth dependence and so that the primary beam dispersion is not taken into account. Boltzmann's equation is numerically solved after its development in partial waves.

In the model proposed by Bindi et al., the diffusion of the primary electrons inside the sample is investigated using a Boltzmann equation treatment in the continuous slowing-down approximation for the energy loss. This treatment developed by Lanteri (75,77,78) generalizes those presented by Bennett and Roth (8) and by Rostaing et al. (108,111). The theoretical results concerning the angular and the energy distribution of the primary electrons as a function of the depth are used for the calculations of the source function.

In all the presented models, the arbitrary distinction between primary and secondary electrons is maintained, the criterion for this being the energy. As commonly admitted, the energy of true SE does not exceed a few tens of electronvolts. It follows that the results are reliable as long as this energy is lower than that of the pri-



mary electrons. Furthermore, excitation and decay of surface plasmon are neglected. The transport theory for kinetic emission of secondary electrons by electron and ion bombardment developed by Schou (113) is more phenomenological. In this model the secondary electron emission is related to the distribution of energy deposited in the target by the primary beam.

#### Simulation models

While elementary processes are well understood both theoretically and experimentally, an analytical treatment of the SEE phenomenon requires many simplifying assumptions. To overcome these difficulties, Bimshas (10) was the first to use a Monte-Carlo simulation method. Cailler and Ganachaud (26,45,46) developed this method in the case of Cu. The principle of this method is to follow the history of an incident electron from the moment it crosses the entrance surface of a solid until its escape back in the vacuum or, alternatively, its absorption in the solid. The simulation consists in applying this principle to a great number of particles.

The use of a uniform distribution of random numbers between 0 and 1 allows one to obtain :

- the path length of the electrons,
- the type of collision whose probability is directly related to the inverse of the m.f.p.,
- the amounts of transferred energy and the angular parameters relative to both exciting and excited electrons.

The number of simulated primary electrons is generally taken between 500 and 10,000. The energy distribution of secondary electrons is obtained in the form of histograms, the width of the classes being generally 1 eV. The ratio of the number of emitted electrons to that of simulated primary electrons gives the yield.

Ganachaud (44,47,48) extended this method to both normal and noble metals. Shimizu and Murata (118) also applied the Monte-Carlo method to somewhat different models for the description of the interaction of primary electrons with solids, in the energy range generally used in electron microscopy. Koshikawa and Shimizu (71), then applied it, in the case of Cu, to the diffusion of secondary electrons created by primary electrons as these penetrate into the solid. As a result, one can calculate  $\delta_0$ , an important parameter for the definition of the image contrast in scanning electron microscopy. Koshikawa et al. (72) also used this method to simulate the shift of the peak and the variation of the f.w.h.m. of the energy distribution curve as a function of the thickness of a layer of beryllium deposited upon a copper substrate.

#### Comparison between theory and experiment

Comparison between results obtained from the different models presented above and experiment is made on two classes of metal : one is aluminium for which the free electron approximation is justified and which has received much attention ; the other is the class of the so-called noble metals (Au, Cu).

We are only interested in those models which enable us to obtain at the same time, energy and

angular distributions, as well as yield. Moreover, it is worth noting that, to our knowledge, only the simulation or the transport models, as developed by Ganachaud (44) or Bindi et al. (13,14), permit one to obtain the true yield of SEE. Previous analytical models and those developed later by Chung and Everhart (30) and Rösler and Brauer (106,107), treat only the primary electron contribution to SEE, during penetration into the solid, leading to the yield  $\delta_0$ . With the help of some simplifying assumptions, Bindi et al.'s model (15) can also give some rough estimation of  $\delta_0$ . Results for Al

Energy distribution. Experimentally, for primary energies in the range 0.6 keV - 2 keV, the main energy distribution features (peak position, f.w.h.m.) vary only slightly. Peak position is situated between 1.5 and 2 eV, and f.w.h.m. varies between 6 and 9 eV (12,38,105).

All the energy distributions reveal the existence of a fine structure by the appearance of a shoulder around 10.5 eV. Another shoulder at 5.5 eV can only be seen for energies lower than about 300 eV. These structures are generally attributed to bulk and surface plasmon decay (56, 59,64,65,105).

Energy distribution curves given by the different transport models are shown, as normalized in figure 6, and in real size in figure 7. One can see from these figures that, with the exception of Amelio's analytical results, the theoretical energy distribution curves are in good agreement with experiment.

On figure 8, we compare the energy distribution given by our model, with that of Ganachaud's simulation model (44) with physical assumptions very close to ours. Peak positions being the same, differences in f.w.h.m. are attributed essentially to the surface plasmon decay, included in the simulation model.

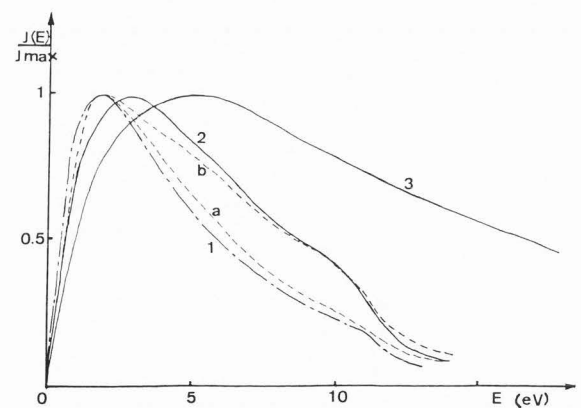


Figure 6. Comparison of theoretical and experimental normalized secondary electron energy distribution curve of Al ( $E_{p0} = 1$  keV). Theoretical spectra 1 : our model (13) ; 2 : Chung and Everhart's results (30) ; 3 : Amelio's model with correction (2). Experimental spectra : a : our results (12) ; b : Roptin (105).

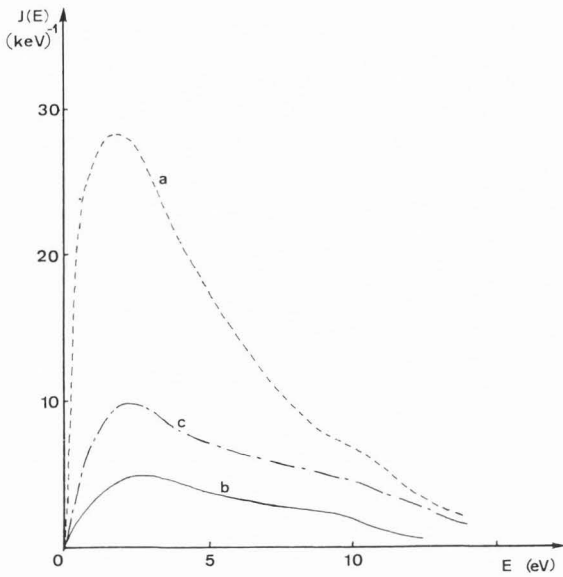


Figure 7. Theoretical secondary electron energy distribution of Al ( $E_{p0} = 2$  keV). a : our model (11) ; b : Chung and Everhart (30) ; c : Rösler and Brauer (107).

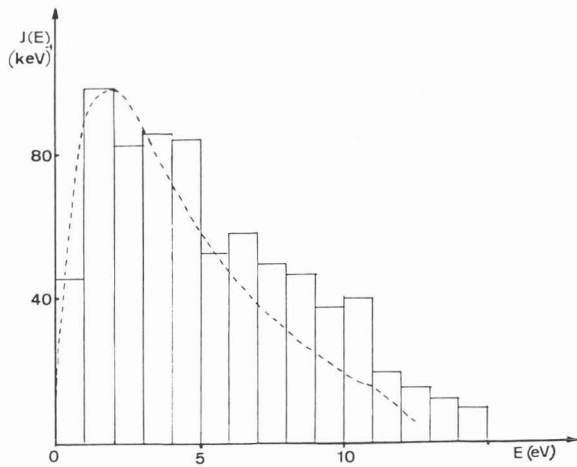


Figure 8. Energy distribution of secondary electrons of Aluminium ( $E_{p0} = 0.6$  keV). Curve : our model (11) ; Histogram : Ganachaud (48).

One can see, from the above comparisons, the fundamental importance of taking into account both the contribution of the plasmon decay in the source function (in addition to individual interactions) and the energy dependence of the m.f.p.

Angular distributions of true SE. Ganachaud's simulation model (44), our model (13,14) and that of Rösler and Brauer (106,107), give results in very good agreement with the experimental distribution. The same good agreement is also obtained

when the internal secondary electron excitation presents a strong anisotropy (individual excitation). This is nothing else but an isotropic internal distribution resulting essentially from elastic collisions.

Yield. As previously mentioned, the true secondary emission yield, can only be obtained by models taking into account the energy and angular dispersion of primary beams.

In table 2, we present Ganachaud's (44) theoretical values of  $\delta_{true}$ , those obtained by our model as well as the experimental values. In table 3, we present theoretical as well as experimental values of  $\delta_0$ . Generally, a good agreement is observed except for the Chung and Everhart's model which shows an important absorption probably due to an oversimplified description of the internal secondary electrons transport process.

Table 2. Secondary electron yield  $\delta_{true}$  for Al

$E_{p0}$ (keV)	0.4	0.6	1	1.2	2	Ref
Theory	0.77	0.62	0.38	0.32	0.18	(11)
	0.83	0.68				(44)
Experiment	0.77	0.72	0.57	0.52	0.39	(11)
	0.66	0.59	0.45	0.41	0.23	(18)
	0.68	0.61	0.48	0.46		(105)

Table 3. Secondary yield  $\delta_0$  for Al produced by the incident primary electron.

$E_{p0}$ (keV)	0.6	1	1.2	1.5	2	Ref
Theory	0.34	0.21	0.18	0.14		(11)(15)
					0.10	(107)
		0.051			0.08	(107)
Experiment			0.15		0.13	(18)
	0.26	0.25	0.22	0.21		(79)

Results for noble metals (Cu, Au)

These metals have been investigated less than Al. Among the different theoretical models proposed for SEE in Cu and Au, we can mention :  
 - Cailler's (27) transport model based on the works of Wolff and Puff. In this model, the source function takes into account the presence of "d" electrons in these metals ; the dielectric function is obtained from the optical spectra and an empirical m.f.p. is used in the transport of

excited electrons.

- Amelio's transport model including corrections suggested by Moulin et al. (89). The source function is that of Streitwolf restricted to individual interactions.
- Bindi's et al. (14) transport model adopting the same source function as Cailler.
- Koshikawa and Shimizu's simulation model (71) using Streitwolf's source function, and also experimental m.f.p. for the cascade mechanism. Here, the primary beams dispersion is neglected.
- Ganachaud's simulation model (44).

Energy distributions. Normalized energy distributions given by models of Cailler, Amelio and Koshikawa and Shimizu in the case of copper are shown in figure 9 for 0.2, 0.6 and 1 keV primary energies respectively. The normalized energy distributions given by models of Ganachaud and Bindi et al. for the same metal, are shown in figure 10.

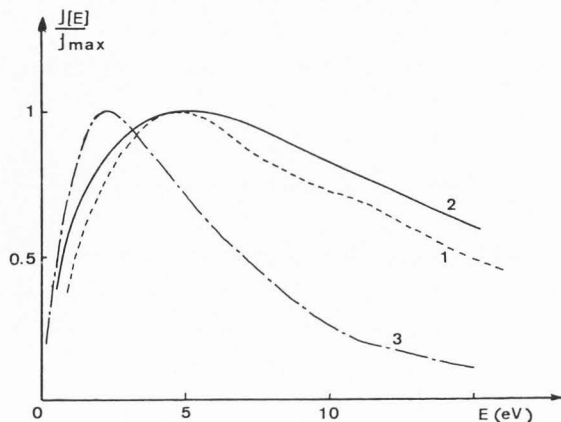


Figure 9. Normalized secondary electron energy distribution for copper. 1 : Cailler (27) for  $E_{p0} = 0.2$  keV ; 2 : Amelio's model (2) with correction for  $E_{p0} = 0.6$  ; 3 : Koshikawa and Shimizu (71) for  $E_{p0} = 1$  keV.

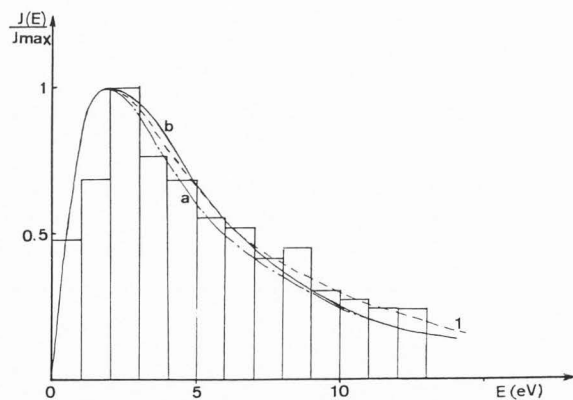


Figure 10. Normalized secondary electron energy distribution for copper ( $E_{p0} = 1$  keV). 1 : our model (14) ; histogram : Ganachaud (44). Experimental curves : a : our results - b : Roptin quoted by Ganachaud (44).

In table 4, we grouped the experimental values of the energy distribution features for the previously mentioned primary energies. The marked fine structure initially observed by Scheibner and Tharp (112) in the neighbourhood of 13 eV for Cu was not confirmed by the later measurements of Koshikawa and Shimizu (70), Pillon (93) and Bindi et al. (12).

Table 4. Peak position ( $E_{max}$ ) and full width at half-maximum of the secondary electron energy distribution for copper at primary energy  $E_{p0} = 0.2; 0.6 ; 1$  keV.

$E_{p0}$ (keV)	0.2	0.6	1	Ref
$E_{max}$ (eV)	1.7	1.6	1.5	(11)
	2.3	2.1	1.9	(44)
			1.4	(71)
f.w.h.m. (eV)	6.2	5.7	5.2	(11)
	8.4	7.1	6	(44)
			5.4	(71)

In figure 11, we show, in a reduced form, the SE energy distributions for gold, given by the theoretical models of Ganachaud (44) and Bindi et al. (13,14) as well as the experimental results of Bindi et al. (12) and of Pillon and Roptin, published in (44). The latter authors observed a hump near about 10 eV.

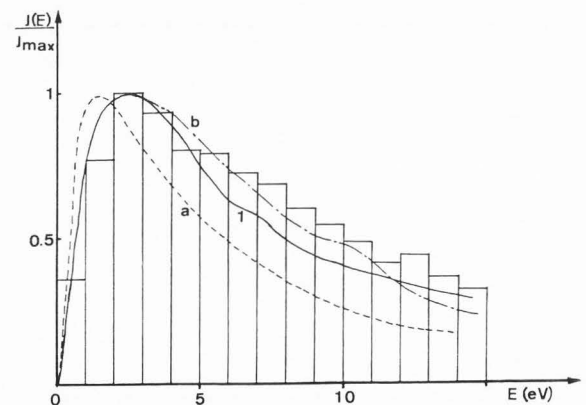


Figure 11. Normalized secondary electron energy distribution for gold ( $E_{p0} = 0.6$  keV). 1 : our model (12) ; Ganachaud (44) : histogram. Experimental curves : a : our results (12) - b : Pillon and Roptin quoted by Ganachaud (44).

Examining figures 9, 10, 11 and table 4, one can see that the energy distribution features (f.w.h.m. and peak position) given by theoretical

## Secondary electron emission

models of Koshikawa and Shimizu (71), Ganachaud (44) and Bindi et al. (12) are in very good agreement with the experimental results.

The fine structures found in some energy distributions are to be attributed to those in the loss functions if one takes into account the more or less important inelastic collision rates, which are connected to the m.f.p. values.

SEE yield. The values of the contribution  $\delta_0$  of the incoming primary electrons in the 1-2 keV energy range are about 0.25 for Cu and 0.4 for Au (79). Among the models previously mentioned, giving  $\delta_0$ , only that of Cailler leads to a correct value, provided an empirical value of the m.f.p. is used; this is particularly important for copper. The model of Koshikawa and Shimizu (71) using the Streitwolf's source function gives values of  $\delta_0$  which are too low. Correct values of the true SE yield are only given by Ganachaud's theoretical model. For a primary energy  $E_{p0} = 0.6$  keV, the values of  $\delta_{true}$  are situated between 1.25 and 1.42 for gold, and between 0.9 and 1.1 for Cu. Values of  $\delta_{true}$  given by the model of Bindi et al. (13,14) are five times too low for these metals.

### Conclusion

From the above comparison between theory and experiments we can determine the specific conditions which will allow a theoretical model of SEE to give full account of the experimental data.

First, concerning the energy and angular distributions, inelastic and elastic interactions of internal SE must be correctly described, the energy dependence of m.f.p. being an absolute prerequisite.

Second, concerning the true SE yield, reasonable values will be reached if we take into account all the intrinsic properties of the investigated material, which also give fine structures in the energy distribution curves and equally, the energy and angular dispersion of the incident beam, i.e., the influence of the backscattered electrons on SEE. This last point could explain the low values of the yield given by Bindi et al. transport model (13,14) in noble metals, and the existing discrepancy with Ganachaud's  $\delta_{true}$  values (44).

In fact, in Bindi's model, the energy and angular dispersion of the incident beam in the continuous slowing down approximation, does not permit one to find a correct value of the backscattering coefficient in noble metals, while this approximation appears to be satisfactory for Al.

This is why we have recently developed (80, 109,110) a theoretical model, based on the transport equation, for the analysis of the different processes of electron diffusion, as well as for the analysis of backscattering and transmission in metals. This model takes into account separately all the electron-solid scattering processes and requires only a knowledge of the differential cross section related to these processes. The advantage in the development of such a model is not only restricted to the sole determination of the internal SE excitation, but extends equal-

ly well to other fields such as electron microscopy and Auger electron spectroscopy, as illustrated by the works of Father and Rez (39), Shimizu and Ichimura (117), Fitting and Reinhardt (43), Tofterup (124), Tougart and Sigmund (125), with which our model should be compared.

### Acknowledgements

We are grateful to C. Paparoditis for the translation of this paper.

### Symbol Table

SEE	Secondary electron emission
$\delta_{tot}$	Total SEE yield
$\delta_{true}$	True SEE yield
$\eta$	Backscattering coefficient of primary electrons
$E_{p0}$	Incident primary electrons energy (keV)
$E_p$	Primary electrons energy (keV)
$\delta_0$	SEE yield of forward primary electrons
$\delta_1$	SEE yield of backward primary electrons
C	Mean backscattered electrons effectiveness for SEE
$\hbar\omega$	Transfer of energy (eV)
$\hbar q$	Momentum transfer (N.s)
$\epsilon$	Dielectric function
$\epsilon_1$	Real part of $\epsilon$
$\epsilon_2$	Imaginary part of $\epsilon$
y	Reduced energy transfer
z	Reduced Momentum transfer
$z_c$	Cutoff value of z for plasmon excitation
$\hbar k_F$	Fermi momentum (N.s)
$E_F$	Fermi energy (eV)
E, $E_0$	Electron energy (eV)
W	Probability for an electron to yield an amount of energy $\hbar\omega$ and momentum $\hbar q$ to the solid ( $s^{-1}$ )
e	Electronic charge (Coulombs)
K, L, M	Inner-shells
$L_1, L_{23}$	Inner-subshells
nl	Inner-shell subscript
$\sigma, \sigma_{el}$	Scattering cross section ( $cm^2$ )
$Z_{nl}$	Number of electrons of the nl shell
b, c	Parameters
$E_{nl}$	Binding Energy for the nl shell
$U_{nl}$	Reduced energy
Z	Atomic number
$\Delta E$	Energy loss (eV)
$\sigma_0$	$(eV)^2 (nm)^2$
X	Reduced Energy
y	Reduced energy loss
$\alpha$	Elastic scattering angle
$\xi$	Screening parameter
x	Depth (nm)
v	Electron velocity ( $nm s^{-1}$ )
$\theta$	Angle between the propagation direction and the inward normal
m.f.p.	Mean free path (nm)
f.w.h.m.	Full width at half maximum (eV)
J	Differential normalized density of SEE current ( $keV^{-1}$ )

## References

1. Amelio G.F (1969) "Auger electron spectroscopy and secondary emission in semiconductors" Ph. D. Thesis - Georgia Institute of Technology.
2. Amelio G.F (1970) "Theory for the energy distribution of secondary electrons" J. of Vac. Sci. and Technology 7, 593-604.
3. Ashley J.C, Ritchie R.H (1974) "The influence of plasmon damping on the mean free path of electrons for plasmon excitation" Phys. Stat. Solid (b) 62, 253-260.
4. Ashley J.C, Tung C.J, Ritchie R.H (1975) "Electron interaction cross section in Al and Al<sub>2</sub>O<sub>3</sub>" I.E.E.E Trans. on Nucl. Sci. NS 22, 2533-2536.
5. Ashley J.C, Tung C.J, Ritchie R.H (1979) "Electron inelastic mean free paths and energy losses in solids" Surface Science 81, 409-426.
6. Baroody E.M (1950) "A theory of secondary electron emission from metals" Phys. Rev. 78, 780-786.
7. Beaglehole D. (1965) "Optical properties of copper and gold in the vacuum ultra-violet" Proc. Phys. Soc. 85, 1007-1020.
8. Bennett A.J, Roth L.M (1972) "Effect of primary electron diffusion on secondary electron emission" Phys. Rev. B, 5, 4309-4324.
9. Bethe H. (1930) "Zur theorie des durchgangs schneller korpuskulars trahlen durch materie" Ann. d. Physik 5, 325-400.
10. Bimshaš G. (1961) "Zur theorie der sekundärelektronen emission by metallen" Z. Physik 161, 190-204.
11. Bindi R. (1978) "Contribution à l'étude de l'émission électronique secondaire de cibles métalliques polycristallines" Thèse d'Etat - Université de Nice, France.
12. Bindi R, Lanteri H, Rostaing P. (1979) "Distributions énergétiques expérimentales des électrons secondaires émis par des cibles évaporées d'aluminium, de cuivre, d'or et d'argent" J. Electron. Spect. and Rel. Phen. 17, 249-258.
13. Bindi R, Lanteri H, Rostaing P. (1980) "A new approach and resolution method of the Boltzmann equation applied to secondary electron emission, by reflection for polycrystalline Al" J. Phys. D. Appl. Phys. 13, 267-280.
14. Bindi R, Lanteri H, Rostaing P. (1980) "Application of the Boltzmann equation to secondary electron emission from Cu and Au" J. Phys. D. - Appl. Phys. 13, 461-470.
15. Bindi R, Lanteri H, Rostaing P, Keller P. (1980) "Theoretical efficiency of backscattered electrons in secondary electron emission from Al" J. Phys. D - Appl. Phys. 13, 2351-2361.
16. Bronshtein I.M, Denisov S.S (1965) "Effect of the work function on parameters of secondary electron emission" Sov. Phys. Solid State, 6, 1515-1518.
17. Bronshtein I.M, Denisov S.S (1967) "Secondary electron emission of Al and Ni for obliquely incident primary electrons" Sov. Phys. Solid State, 9, 731-732.
18. Bronshtein I.M, Fraiman B.S (1961) "Inelastic scattering of electrons and secondary electron emission from certain metals and semiconductors" Sov. Phys. Solid State, 3, 1188-1196.
19. Bronshtein I.M, Fraiman B.S (1962) "Secondary electron emission from some solid bodies" Sov. Phys. Solid State, 3, 2087-2088.
20. Bronshtein I.M, Fraiman B.S (1969) "Emission électronique secondaire" Ed. Naouka (Moscow).
21. Bronshtein I.M, Segal R.B (1960) "Inelastic scattering of electrons and secondary electron emission in certain metals I" Sov. Phys. Solid State, 1, 1365-1374.
22. Bronshtein I.M, Segal R.B (1960) "Inelastic scattering of electrons and secondary electron emission in certain metals II" Sov. Phys. Solid State, 1, 1375-1382.
23. Brošens F, Devreese J.T (1980) "Dielectric function of the electron gas with dynamical exchange decoupling" Phys. Rev. B, 21, 1363-1379.
24. Bruining H (1954) "Physics and applications of secondary electron emission" Mac. Graw - Hill Ed. (New-York).
25. Burgess A, Percival I.C (1968) "Classical theory of atomic scattering" in "Advances in atomic and molecular physics" Edited by Bates D.R and Estermann C. 4, 109-141.
26. Cailler M, Ganachaud J.P (1972) "Quelques aspects theoriques de l'émission électronique secondaire du cuivre produite par bombardement d'électrons de faible énergie" Journal de Physique, 33, 903-913.
27. Cailler M. (1969) "Contribution à l'étude théorique de l'émission électronique secondaire induite par bombardement électronique" Thèse d'Etat - Université de Nantes, France.
28. Chung M.S (1975) "Improved calculations of secondary electron energy distribution in metals" J. Appl. Phys. 46, 465-466.
29. Chung M.S, Everhart T.E (1974) "Simple calculation of energy distribution of low energy secondary electrons emitted from metals under electron bombardment" J. Appl. Phys. 45, 707-709.
30. Chung M.S, Everhart T.E (1977) "Role of plasmon decay in secondary electron emission in the nearly free electron metal - Application to Al" Phys. Rev. B, 15, 4699-4715.
31. Dangerfield G.R, Spicer B.M (1975) "K-shell ionization by relativistic electrons" J. of Physics B, 8, 1744-1751.
32. Dekker A.J (1958) "Secondary electron emission" Solid State Physics - Academic Press (New-York).
33. Dekker A.J, Van der Ziel A. (1952) "Theory of the production of secondary emission in solids" Phys. Rev. 86, 755-760.
34. Devreese J.T, Brosens F, Lemmens L.F (1980) "Dielectric function of the electron gas with dynamical exchange decoupling. I Analytical treatment" Phys. Rev. B, 21, 1349-1362.
35. Dionne G.F (1973) "Effects of secondary electron scattering on secondary emission yield curves" J. Appl. Phys. 44, 5361-5364.
36. Drawin H.W. (1961) "Zur formelmässigen darstellung der ionisierungquerschnitte gegenüber elektronenstoss" Z. Physik, 164, 513-521.
37. Estrade G. (1977) "Simulation de l'ionisation interne produite par des électrons, et de la réorganisation électronique consécutive" Thèse de spécialité - Université de Toulouse, France.
38. Everhart T.E, Saeki N, Shimizu R, Koshikawa T. (1976) "Measurement of structure in the energy distribution of slow secondary electrons from Aluminium" J. Appl. Phys. 47, 2941-2945.

39. Fathers D.J, Rez P. (1979) "A transport equation theory of electron backscattering" *Scanning Electron Microsc.* 1979; I: 55-66.
40. Feldkamp L.A, Davis L.C, Stearns M.B (1977) "Analysis of electron inelastic scattering data with applications to Cu" *Phys. Rev. B* 15, 5535-5544.
41. Fischbeck H.J (1966) "Über die Anregung von rumpfelektronen durch stoss mit schnellen primärelektronen in metallen" *Phys. Stat. Sol.* 15, 387-398.
42. Fitting H.J (1974) "Transmission energy distribution, and SE excitation of fast electrons in thin solid films" *Phys. Stat. Sol. (a)* 26, 525-535
43. Fitting H.J, Reinhardt J. (1985) "Monte Carlo simulation of keV electron scattering in solid targets" *Phys. Stat. Sol. (a)* 88, 245-259.
44. Ganachaud J.P (1977) "Contribution à l'étude théorique de l'émission électronique secondaire des métaux" Thèse d'Etat, Université de Nantes, France.
45. Ganachaud J.P, Cailler M. (1973) "Traitement unifié de l'émission électronique secondaire du cuivre par une méthode de Monte Carlo" *J. de Physique*, 34, 91-98.
46. Ganachaud J.P, Cailler M. (1973) "Description d'un modèle d'émission électronique secondaire prenant en compte collisions élastiques et inélastiques" *C.R. Acad. Sci. (Paris)* 276, 543-546.
47. Ganachaud J.P, Cailler M. (1979) "A Monte Carlo calculation of the secondary electron emission of normal metals. I The model" *Surf. Sci.* 83, 498-518.
48. Ganachaud J.P, Cailler M. (1979) "A Monte Carlo calculation of the secondary electron emission of normal metals. II Results for Al" *Surf. Sci.* 83, 519-530.
49. Gibbons D.J (1966) "Secondary electron emission" *Handbook of Vacuum Physics*, Vol 2, Part 3, 300-395, Ed. H. Beck, Pergamon Press, Oxford, U.K.
50. Gorobchenko V.D, Maksimov E.G (1980) "The dielectric constant of an interacting electron gas" *Sov. Phys. Usp.* 23, 35-58.
51. Grinchak A.I (1966) "Interaction of secondary electrons with a solid state plasma" *Sov. Phys. Solid State*, 8, 1000-1001.
52. Gryzinski M. (1965) "Two particles collisions. I. General relations for collisions in the laboratory system" *Phys. Rev.* 138, 305-321.
53. Gryzinski M. (1965) "Two particles collisions. II. Coulomb collision in the laboratory system of coordinates" *Phys. Rev.* 138, 322-335.
54. Gryzinski M. (1965) "Classical theory of atomic collisions. I. Theory of inelastic collisions" *Phys. Rev.* 138, 336-358.
55. Guba A.I (1962) "The energy-angular distribution of secondary electrons during secondary electron emission" *Sov. Phys. Solid State*, 4, 1197-1199.
56. Guennou H, Dufour G, Bonnelle C. (1974) "Emission électronique secondaire de cibles solides d'Al et Mg" *Surf. Sci.* 41, 547-554.
57. Hachenberg O, Brauer W. (1954) "Der gegenwärtige stand der theorie der sekundärelektronen emission" *Fortschritte der Physik*, 1, 439-485.
58. Haymann P. (1962) "Emission électronique secondaire" *Journal de Recherches du CNRS*, 61, 357-374.
59. Henrich V.E (1973) "Role of bulk and surface plasmon in the emission of slow secondary electrons : polycrystalline Aluminium" *Phys. Rev. B* 7, 3512-3519.
60. Hink W, Ziegler Z. (1969) "Der wirkungsquerschnitt für die ionisierung der K-Schale von Al durch elektronenstoss (3-30 keV)" *Z. Physik*, 226, 222-234.
61. Ichimura S, Aramata M, Shimizu R. (1980) "Monte Carlo calculation approach to quantitative Auger electron spectroscopy" *J. Appl. Phys.* 51, 2853-2860.
62. Jahrreiss H. (1972) "Secondary electron emission from thin films" *Thin Solid Films*, 12, 187-200.
63. Jahrreiss H, Oppel W. (1972) "Angular distributions of secondary electrons originating from thin films of different metals in re-emission and transmission" *J. Vac. Sci. Technol.* 9, 173-176.
64. Jenkins L.H, Chung M.F (1971) "The energy spectrum of back-scattered electrons and characteristic loss and gain phenomena of the Cu (111) Surface" *Surface Sci.* 26, 151-164.
65. Jenkins L.H, Chung M.F (1971) "Auger and other characteristic energies in secondary electron spectra from Al surfaces" *Surface Sci.* 28, 409-422.
66. Jonker J.L (1951) "The angular distribution of the secondary electrons of Nickel" *Philips Res. Rep.* 6, 372-387.
67. Jonker J.L (1952) "On the theory of secondary electron emission" *Philips Res. Rep.* 7, 1-20.
68. Kanter H. (1961) "Contribution to backscattered electrons to secondary electron formation" *Phys. Rev.* 121, 681-684.
69. Kliever K.L, Fuchs R (1969) "Lindhard dielectric functions with a finite electron lifetime" *Phys. Rev.* 181, 552-558.
70. Koshikawa T, Shimizu R. (1973) "Secondary electron and backscattering measurements for polycrystalline copper with a spherical retarding field analyser" *J. Phys. D - Appl. Phys.* 6, 1369-1380.
71. Koshikawa T, Shimizu R. (1974) "A Monte Carlo calculation of low energy secondary electron emission from metals" *J. Phys. D - Appl. Phys.* 7, 1303-1315.
72. Koshikawa T, Goto K, Shimizu R, Ishikawa K. (1974) "Secondary electron energy spectra from Be layer evaporated on Cu" *J. Phys. D - Appl. Phys.* 7, L174-L177.
73. Krefting E.R, Reimer L. (1973) "Quantitative analysis with microprobe and secondary ion mass spectroscopy" Ed. E. Preuss (Zentralbibliothek der K.F.A. Jülich GmbH. p. 114.
74. Landau L, Lifchitz E. (1967) "Quantum mechanics" Ed. Mir (Moscow).
75. Lanteri H. (1978) "Contribution à l'étude de la transmission d'électrons d'énergie inférieure à 3 keV à travers des cibles d'Al, Ag, Cu" Thèse d'Etat, Université de Nice, France.
76. Lanteri H, Bindi R, Rostaing P. (1977) "Effects of the working conditions of retarding field spectrometers on the energy distribution of secondary electrons" *J. Elect. Spect. and Rel. Phen.* 12, 451-458.

77. Lanteri H, Bindi R, Rostaing P. (1981) "Application of splitting-up method to the numerical treatment of transport equation. Analysis of the transmission of electrons through thin self supporting metallic targets" *J. Comput. Phys.* **39**, 22-44.
78. Lanteri H, Bindi R, Rostaing P. (1982) "Modele theorique de la transmission et de la retrodiffusion d'électrons dans des cibles métalliques minces ou semi-infinies : Application à l'Al, Ag et Cu" *Thin Solid Films*, **88**, 309-333.
79. Lanteri H, Richard C, Bindi R, Keller P (1975) "Détermination expérimentale de l'efficacité des électrons retrodiffusés dans l'émission électronique secondaire de Au et Al" *Thin Solid Films*, **27**, 301-310.
80. Lanteri H, Rostaing P, Bindi R. (1986) "Application du modèle théorique à l'étude des pertes d'énergie caractéristiques des électrons transmis et retrodiffusés dans le cas de l'Aluminium" *Thin Solid Films*, **135**, 289-299.
81. Lindhard J. (1954) "On the properties of a gas of charged particles" *Kgl. Danske Videnskab Selskab Mat. Fys. Medd* **28**, 8-57.
82. Lotz W. (1967) "An empirical formula for the electron impact ionization cross section" *Z. Physik*, **206**, 205-211.
83. Lye R.G, Dekker A.J (1957) "Theory of secondary emission" *Phys. Rev.* **107**, 977-981.
84. Mac Guire E.J (1971) "Kand L shell fluorescence and Auger yields and Auger electron spectroscopy" *J. Phys. (Paris) C4*, **32**, 124-127.
85. Manson S.T (1972) "Inelastic collisions of fast charged particles with atoms. Ionization of the Aluminium L shell" *Phys. Rev. A*, **6**, 1013-1024.
86. Marshak R.E (1947) "Theory of slowing down of neutrons by elastic collision with atomic nuclei" *Rev. Mod. Phys.* **19**, 185-238.
87. Mayer H, Hölzt J. (1966) "Détermination expérimentale de la profondeur maximale d'extraction des électrons secondaires monocinétiques" *Phys. Stat. Solidi*, **18**, 779-785.
88. Mermin N.D (1970) "Lindhard dielectric function in the relaxation time approximation" *Phys. Rev. B*, **1**, 2362-2363.
89. Moulin B, Ganachaud J.P, Cailler M. (1973) "Considérations sur l'importance de quelques hypothèses physiques dans la théorie de l'émission électronique secondaire" *Phys. Stat. Solidi (b)* **59**, 79-85.
90. Nagel S.R, Witten T.A (1975) "Local field effects on inelastic electron scattering" *Phys. Rev. B*, **11**, 1623-1635.
91. Noiray J.C, Bindi R, Lanteri H, Martin F, Borgnino J. (1974) "Détermination de la profondeur d'origine d'électrons secondaires vrais dans l'Or et l'Aluminium" *Thin Solid Films*, **23**, 63-73.
92. Palmberg P.W (1966) "Electron diffraction and secondary emission studies on Sodium-covered Germanium" *Dissert. Abstract B (USA)* **37**, 1261-1261.
93. Pillon J. (1974) "Etude critique d'un spectroscope Auger pour l'émission électronique secondaire - Résultats obtenus sur un cristal de Cu (111)" Thèse de Docteur-Ingénieur, Université de Nantes, France.
94. Pines P. (1964) "Elementary excitations in solids" W.A. Pergamon Inc. New-York.
95. Powell B.P, Woodruff D.P (1972) "Plasmon effects in electron energy loss and gain spectra in Aluminium" *Surf. Sci.* **33**, 437-444.
96. Powell C.J (1976) "Cross sections for ionization of inner-shell electrons by electrons" *Rev. Mod. Phys.* **48**, 33-47.
97. Puff M. (1964) "Zur theorie der sekundärelektronenemission. Der transportprozess. I." *Phys. Stat. Solidi*, **4**, 125-138.
98. Puff M. (1964) "Zur theorie der sekundärelektronenemission. Der transportprozess. II." *Phys. Stat. Solidi*, **4**, 365-382.
99. Puff M. (1964) "Zur theorie der sekundärelektronenemission. Der transportprozess. III." *Phys. Stat. Solidi*, **4**, 569-586.
100. Quinn J.J (1962) "Range of excited electrons in metals" *Phys. Rev.* **126**, 1453-1457.
101. Raether H. (1965) "Solid state excitations by electrons" *Springer tracts Mod. Phys.* **38**, 84-156.
102. Richard C. (1974) "Contribution à l'étude de l'émission électronique secondaire par bombardement électronique, sur des cibles d'Al et Au" Thèse de Spécialité - Université de Marseille, France.
103. Richard C, Bindi R, Lanteri H, Keller P. (1975) "Rendement d'émission électronique secondaire déduit d'un modèle analytique : comparaison avec les valeurs expérimentales pour Au et Al" *Thin Solid Films*, **26**, 119-127.
104. Ritchie R.H, Ashley J.C (1965) "The interaction of hot electrons with free electron gas" *J. Phys. Chem. Solids*, **26**, 1689-1694.
105. Roptin D. (1975) "Étude expérimentale de l'émission électronique secondaire de l'Aluminium et de l'Argent" Thèse de Docteur-Ingénieur, Université de Nantes, France.
106. Rösler M, Brauer W. (1981) "Theory of secondary electron emission. I. General theory for nearly free electron metals" *Phys. Stat. Solidi (b)* **104**, 161-175.
107. Rösler M, Brauer W. (1981) "Theory of secondary electron emission. II. Application to Aluminium" *Phys. Stat. Solidi (b)* **104**, 575-587.
108. Rostaing P. (1977) "Contribution à l'étude expérimentale et théorique de la transmission d'électrons à travers des cibles minces d'Aluminium" Thèse de Spécialité, Université de Nice, France.
109. Rostaing P. (1983) "Modèle théorique de la diffusion d'électrons de faible énergie dans les métaux" Thèse d'Etat, Université de Nice, France.
110. Rostaing P, Bindi R, Lanteri H. (1986) "Modèle théorique pour l'analyse des différents processus de diffusion des électrons dans les métaux" *Thin Solid Films*, **135**, 277-289.
111. Rostaing P, Lanteri H, Bindi R. (1977) "Etude expérimentale de la transmission d'électrons d'énergie inférieure à 3 keV à travers des lames minces d'Aluminium sans support" *Thin Solid Films* **46**, 81-91.
112. Scheibner E.J, Tharp L.N (1967) "Inelastic scattering of low energy electrons from surfaces" *Surf. Sci.* **8**, 247-265.
113. Schou J. (1980) "Transport theory for kinetic emission of secondary electrons from solids" *Phys. Rev. B*, **22**, 2141-2174.

114. Seif S.A.H, Berenyi D, Bybok G.Y (1974) "Inner shell ionization cross sections for relativistic electrons" *Z. Physik*, **267**, 169-172.
115. Sharif N. (1976) "Réalisation d'un analyseur cylindrique de vitesses d'électrons : Application à l'étude de la transmission des électrons à travers des lames minces d'Aluminium" Thèse de Spécialité, Université de Marseille III, France.
116. Shimizu R. (1974) "Secondary electron yield with primary electron beam of kilo-electron volts" *J. Appl. Phys.* **45**, 2107-2111.
117. Shimizu R, Ichimura S. (1983) "Direct Monte Carlo simulation of scattering processes of keV electrons in Aluminium : comparison of theoretical  $N(E)$  spectra with experiment" *Surf. Sci.* **133**, 250-266.
118. Shimizu R, Murata K. (1971) "Monte Carlo simulation of electron sample interactions in the scanning electron microscope" *J. Appl. Phys.* **42**, 387-394.
119. Singwi K.S, Sjolander A, Tosi M.P, Land R.N (1970) "Electron correlation at metallic densities. IV" *Phys. Rev. B*, **1**, 1044-1053.
120. Singwi K.S, Tosi M.P, Land R.N, Sjolander A. (1968) "Electron correlation at metallic densities" *Phys. Rev.* **176**, 589-599.
121. Stolz H. (1959) "Zur theorie der sekundärelektronenemission von metallen. Der transportprozess" *Ann. d. Phys.* **3**, 197-210.
122. Streitwolf H.W (1959) "Zur theorie der sekundärelektronenemission von metallen. Der anregungsprozess" *Ann. d. Phys.* **3**, 183-196.
123. Thomas S, Pattinson E.B (1970) "Range of electrons and contribution of backscattered electrons in secondary production in Aluminium" *J. Phys. D - Appl. Phys.* **3**, 349-357.
124. Tofterup A.L (1985) "Theoretical aspect of quantitative electron spectroscopy" Thesis - Odense Universitet.
125. Tougart S, Sigmund P. (1982) "Influence of elastic and inelastic scattering on energy spectra of electrons emitted from solids" *Phys. Rev. B*, **25**, 4452-4466.
126. Touzillier L. (1970) "Contribution à l'étude de l'émission électronique secondaire du germanium sous bombardement électronique" Thèse d'Etat, Université de Toulouse, France.
127. Tung C.J, Ritchie R.H (1977) "Electron slowing-down spectra in aluminium metal" *Phys. Rev. B*, **16**, 4302-4313.
128. Valkealahti S, Nieminen R.M (1984) "Monte Carlo calculations of keV electron and position slowing down in solids" *Appl. Phys. A - Solids and Surfaces*, **35**, 51-60.
129. Van der Ziel A. (1953) "A modified theory of production of secondary electrons in solids" *Phys. Rev.* **92**, 35-39.
130. Vriens L. (1966) "Electron exchange in binary encounter collision theory" *Proc. Phys. Soc.* **89**, 13-21.
131. Wehenkel C (1975) "Mise au point d'une nouvelle méthode d'analyse quantitative des spectres de pertes d'énergie d'électrons rapides diffusés dans la direction du faisceau incident : Application à l'étude des métaux nobles" *J. de Physique*, **36**, 199-213.
132. Wolff P.A (1954) "Theory of secondary electron cascade in metals" *Phys. Rev.* **95**, 56-66.
133. Young J.R (1957) "Dissipation of energy by 2.5-10 keV electrons in  $Al_2O_3$ " *J. Appl. Phys.* **28**, 524-525.
134. Zacharias P. (1974) "Behaviour of collective volume excitations in aluminium near the critical wave vector : transitions into single particle excitation" *J. Phys. C - Solid State Physics*, **7**, L26-L27.
135. Zacharias P. (1975) "Behaviour of collective volume excitations in aluminium near the critical wave vector : transitions into single particle excitation" *J. Phys. F - Metal phys.* **5**, 645-656.

#### Discussion with Reviewers

K. Murata : What is the reason why your theoretical values are too low for Cu and Au ? Do you think the backscattering contribution which you neglected in your model is primarily responsible for the discrepancy ?

Authors : The backscattering contribution is not neglected in our model but we find that the scattering and the energy loss of primary electrons in the continuous slowing down approximation give values of  $\eta$  too low in the case of Cu and Au and consequently for the excitation function including this contribution. Furthermore, the excitation function for Cu and Au contains an impact parameter of which the value is of the order of the interatomic distance. Following Cailler we have used 0.14 nm in our calculation but a value of 0.05 nm increases the yield by a factor of two.

We think that these two reasons can explain the low values for Cu and Au.

K. Murata : When you check the validity of the theoretical model, the accuracy of experimental data to compare with is important. However, as you can see, the experimental data deviate often from each other. Could you comment on the accuracy of the data and main factors which determine it ?

Authors : The discrepancy between experimental data results from :

- the nature of the target, i.e, polycrystalline, or single crystal, bulk metal or evaporated layers;
- the nature of the target affect the work function.
- the quality of vacuum.
- the working conditions of the retarding field spectrometers used in measurements of secondary electrons energy distributions. Spurious peaks connected with secondary electron emission from the grids of the spectrometer can appear in the low energy range.

K. Murata : Could you briefly describe your newly developed model ?

Authors : In our newly developed model, the scattering of primary electrons in metals is also described by Boltzmann's transport equation, but not by means of the continuous slowing down approximation. The new formulation takes into account separately all the electron-solid scattering processes. Application of the theoretical model to a given metal requires only a knowledge of the differential cross sections related to these processes.



K. Murata : What do you think of a contribution of fast secondary electrons to the generation of true secondary electrons, which has been investigated by D.C. Joy (J. Microscopy, 136-241 (1984))?  
Authors : The probability of exciting fast secondary electrons by individual interaction is weak. Furthermore, these electrons cannot be distinguished from backscattered primary electrons having lost much energy in the target. In our model the energy limit between fast internal secondary electrons and low primary electrons was fixed at 100 eV. We have verified that greater values do not modify the results.

J. Schou : Could the authors describe more detailed how they include the contribution of the backscattered electrons to the total secondary electron yield in their model ?

Authors : The scattering and the energy loss of primary electrons in the target is described by Boltzmann's equation in the continuous slowing down approximation. So, we obtain the primary electron density  $f(E_p, \Omega_1, x)$  as a function of depth  $x$ , energy  $E_p$  and direction  $\Omega_1$ . The knowledge of  $f$  allows us to obtain the source function:

$$S(E, \Omega, x, E_{p_0}) = \iiint_{E_p(\text{Min})}^{E_{p_0}} S(E, E_p, \Omega_2) \times f(E_p, \Omega_1, x) dE_p d\Omega_1 \quad (13)$$

where  $S(E, E_p, \Omega_2)$  is the excitation source function resulting from electron-electron scattering or volume plasmon decay.

$E$  is the energy of internal secondary electron.  $\Omega$  is the direction of internal secondary electron.  $E_{p_0}$  is the initial incident energy. The source function is used in the transport model of secondary electrons. So, we obtain the true secondary electron yield  $\delta = \delta_0 + \delta_1$ . With the value of  $f$  at  $x = 0$ , we can calculate the backscattering coefficient  $\eta$  and the total secondary yield  $\delta_{\text{Tot}} = \delta + \eta$ .

Z. Radzinski : Have you tried to apply your theory to describe SEE from insulators and semiconductor materials, including compounds. Which element of your theory would be responsible for the high yield of SEE in the case of insulators?

Authors : We have not tried to apply our model for description of SEE from insulators or semiconductor materials. For these materials, the internal electrical field must be taken into account in the transport equation, and another resolution method must be developed. We think that the internal electrical field is partly responsible of the high yield of SEE, together with the high values of m.f.p. in such materials.

Z. Radzinski : Can you say something about the practical usefulness of the models mentioned in this paper? Which category of models is most frequently used and which in your opinion, are more valid and under what circumstances?

Authors : Simulation's models and transport's models give approximately the same results when the elementary processes taken into account are described in a similar way.

However, the simulation's model seems more easy to carry out, but at the expense of computing time if the same precision is required such as for obtaining fine structures.

P. Rez : Although this paper is concerned only with metals would the authors be prepared to comment on both experiment and theory for secondary emission from oxides and semiconductors ?

Authors : We have not investigated the secondary emission from oxides and semiconductors. As mentioned previously, experiment and theory for these materials differ strongly from those concerning metals.

P. Rez : Is it necessary to include exchange terms in the description of inelastic scattering for secondary emission ? I note that most treatments neglect these effects.

Authors : The most complete models presented in this paper show that it is possible to take into account simultaneously all the processes appearing in SEE. In a first step, particularly in transport theories, these processes were described in an oversimplified manner in view of an easier numerical treatment ; that is why the exchange term was neglected.

We can now include this effect in a more realistic description of the inelastic scattering of internal secondary electrons ; Ganachaud (44) showed that the net result was an increase of the individual collisions rate correlated with a decrease of the collective effects for these electrons.

P. Rez : A transport equation approach is semiclassical and neglects the quantum mechanical "wave" nature of the electron which gives rise to diffraction. Is this a serious problem with current theories ? Is it possible for diffraction of low energy secondary electrons to influence any structures observed in the energy distribution ?

Authors : In the model the solid is considered as a set of ions randomly distributed in a free electron gas. This concept precludes any coherent scattering description.